University of Dundee

X-ray irradiation in XTE J1817-330 and the inner radius of the truncated disc in the hard state

Gierliński, Marek; Done, Chris; Page, Kim

[Link to publication in Discovery Research Portal](#)

X-ray irradiation in XTE J1817−330 and the inner radius of the truncated disc in the hard state

Marek Gierliński,[1][*] Chris Done[1] and Kim Page[2]

[1]*Department of Physics, University of Durham, South Road, Durham DH1 3LE*
[2]*Department of Physics and Astronomy, University of Leicester, Leicester LE1 7RH*

ABSTRACT
The key aspect of the very successful truncated disc model for the low/hard X-ray spectral state in black hole binaries is that the geometrically thin disc recedes from the last stable orbit at the transition to this state. This has recently been challenged by direct observations of the low/hard state disc from CCD data. We reanalyse the *Swift* and *RXTE* campaign covering the 2006 outburst of XTE J1817−330, and show that these data actually strongly support the truncated disc model as the transition spectra unambiguously show that the disc begins to recede as the source leaves the disc-dominated soft state. The disc radius inferred for the proper low/hard state is less clear-cut, but we show that the effect of irradiation from the energetically dominant hot plasma leads to an underestimate of the disc radius by a factor of 2–3 in this state. This may also produce the soft excess reported in some hard-state spectra. The inferred radius becomes still larger when the potential difference in stress at the inner boundary, increased colour temperature correction from incomplete thermalization of the irradiation, and loss of observable disc photons from Comptonization in the hot plasma is taken into account. We conclude that the inner disc radius in XTE J1817−330 in the low/hard spectral state is at least six to eight times that seen in the disc-dominated high/soft state, and that recession of the inner disc is the trigger for the soft-hard-state transition, as predicted by the truncated disc models.

Key words: accretion, accretion discs – X-rays: binaries.

1 INTRODUCTION

The accretion flow in black hole binaries (BHB) shows a distinct transition at luminosities of $\sim$0.02–0.2 $L_{\rm Edd}$ (Eddington luminosity). Above this transition, the spectra are soft, peaking at $\sim$1 keV (in νF_ν representation) with a quasi-thermal shape which is well described by models of a geometrically thin, optically thick, cool disc. A series of such disc-dominated spectra from a single object at different mass accretion rates generally shows that the temperature and luminosity of this component vary together as expected for a constant inner radius, as predicted for a thin disc which extends down to the last stable orbit around the black hole, and then spirals quickly in towards the horizon (see e.g. the review by Done, Gierliński & Kubota 2007, hereafter DGK07).

However, below this transition luminosity the spectra are hard, peaking at $\sim$100 keV, entirely unlike the predictions of a standard disc model at these luminosities. There is as yet no clear consensus on the structure of the accretion flow in this low/hard state, but one very attractive solution is that the accretion disc makes a transition to an optically thin, geometrically thick flow. While the detailed prop-

erties of such flows depend on the cooling mechanisms assumed, for example, radiation (Shapiro, Lightman & Eardley 1976), advection (Narayan & Yi 1994), convection (Abramowicz & Igumenshchev 2001) and winds (Blandford & Begelman 1999), they are generically much hotter than a thin disc solution at the same mass accretion rate as they cannot efficiently cool by blackbody radiation (because they are optically thin). These models typically have temperatures around 100 keV, so can match the observations (e.g. the review by Narayan & McClintock 2008, and references therein), and the distinct nature of the hard and soft spectral states has an obvious origin in the very different nature and geometry of the accretion flow.

A key component of this 'truncated disc' model is that the inner disc is replaced by the hot flow. Thus, the inner edge of the cool, thin disc must recede from the last stable orbit as the source transitions from the disc-dominated soft state to the low/hard state. There are several key pieces of evidence supporting this. The spectra in the low/hard state can be roughly described by a power law from 1 to 100 keV, with photon spectral index of 1.5–2. Superimposed on this are clear features from Compton reflection from optically thick, cool material. The solid angle subtended by the reflecting material *correlates* with continuum shape, with harder spectra showing less reflection and less associated fluorescent iron line emission. This is easy to explain in the truncated disc models, as the continuum

[*]E-mail: Marek.Gierlinski@durham.ac.uk

shape is determined by the seed photon luminosity from the disc intercepted by the hot flow, while reflection is determined by the hot flow illuminating the disc. As the disc moves outwards, this gives both fewer soft photons from the disc to Compton cool the flow, and a smaller solid angle of the reflecting material (e.g. Poutanen, Krolik & Ryde 1997; DGK07).

The rapid variability seen in the low/hard state also supports a model with a moving characteristic radius. All the major characteristic frequencies (low-frequency break and low-frequency quasi-periodic oscillation) seen in the broad-band power spectra move, with higher frequencies (smaller characteristic radii) being seen for softer spectra, as predicted by the truncated disc model (e.g. Churazov, Gilfanov & Revnivtsev 2001; DGK07). Even the behaviour of the radio jet can be (phenomenologically) incorporated into these models, with the hot inner flow providing large-scaleheight plasma and magnetic field close to the horizon to power the jet. The collapse of the hot flow as the source makes a transition to the disc-dominated state triggers the collapse of the jet (e.g. Fender, Belloni & Gallo 2004; DGK07).

While these support the truncated disc model, they are indirect measures of the inner radius of the cool, thin disc. But direct observations of the emission from the disc itself are difficult due to the low disc temperature of any disc (truncated or otherwise) at low luminosities, and the problem is compounded by (generally high) interstellar absorption and the relatively high-energy threshold of the most prolific BHB observatory, *Rossi X-ray Timing Explorer* (*RXTE*). None the less, the direct disc emission was convincingly detected in *Hubble Space Telescope*, *Chandra* and *BeppoSAX* observations of the low interstellar absorption system XTE J1118+480. This transient had peak luminosity over an order of magnitude below the transition to the high/soft state so stayed in the low/hard state during its outburst. The temperature and luminosity of the disc emission clearly showed that it was truncated a few hundred Schwarzschild radii from the black hole (Chaty et al. 2003).

Thus, the disc is plainly truncated at very low L/L_{Edd}, but extends down to the last stable orbit in the high/soft state. Therefore, it must start to recede at some point, and the transition is the obvious place. However, Miller, Homan & Miniutti (2006a) and Rykoff et al. (2007, hereafter R07) have claimed that observations of direct disc emission in the low/hard state at luminosities close to the transition show that the disc still extends down to the last stable orbit after the transition, requiring another (as yet unknown) physical mechanism for the transition. Here, we re-examine the data of R07 from XTE J1817−330, as this is the only CCD-based (and hence low-energy instrument threshold) campaign following a BHB outburst with reasonable sampling, and the low interstellar absorption towards this object means that the soft X-ray disc component can be well constrained. Startlingly, the simple disc fits show that the inner disc recedes during the transition, consistent with the truncated disc picture derived above (see also Cabanac et al., in preparation). However, the apparent radius then *decreases* as the source enters the low/hard state, back to a value consistent with that seen in the high/soft state (see also R07). However, we show that the apparent radius in the low/hard state can be underestimated by a large factor through the effects of X-ray irradiation (which also changes the colour temperature correction from that expected in the high/soft state), together with the changing stress condition at the inner boundary and suppression of the observed seed photons by Compton scattering. Thus, the low/hard state in XTE J1817−330 is also consistent with a truncated disc, and this physical mechanism can also explain the apparently small radii for the inner disc seen in other objects (e.g. Miller et al. 2006a). However, irrespective of

the detailed models used for the low/hard state, the transition spectra *always* show that the disc inner radius is larger than that in the high/soft state, giving strong confirmation that disc truncation is the physical origin of the soft–hard-state transition.

2 DATA REDUCTION

RXTE observed XTE J1817−330 from 2006 January 27 to August 2. We reduced these data using FTOOLS version 6.4. We extracted energy spectra from detector 2 (top layer only) of the Proportional Counter Array (PCA), and added 1 per cent systematic error in each channel. We use these data for spectral fitting in 3–20 keV band. We also extracted power density spectra (PDS) from all available detectors in full PCA energy band (2–60 keV) and 1/256–64 Hz frequency band.

The source was very bright at the start of the outburst, so the *Swift* X-ray Telescope (XRT) was in Windowed Timing mode. However, even this was piled up above 100 counts s^{-1} so we extracted these spectra similarly to R07 by excluding the inner, piled up region as determined from where the ratio of grade 0 to grade 0–2 events becomes constant. This was a 7 pixels radius region for the brightest spectra 1–10, then 2 pixels for spectrum 11 and none for spectra 12–17 (observation numbers as in table 1 of R07). The XRT was switched into Photon Counting mode as the source was so much dimmer, though again pileup became an issue above 0.6 counts s^{-1} so the exclusion region was 5, 3 and 4 pixels for spectra 18, 19–21 and 22, respectively.

3 RESULTS

3.1 Spectral states

Fig. 1 shows the light curve and hardness-intensity diagram (HID) of all 150 PCA observations, where hardness is the ratio of count rate in the 6.3–10.5 to 3.8–6.3 keV energy bands (e.g. Fender et al. 2004). In order to better understand spectral evolution of XTE J1817−330 during its outburst, we fitted all the PCA data with a simple model, consisting of disc and Comptonization. The disc is modelled by standard DISKBB model, while the high-energy tail by thermal Comptonization code THCOMP[1] (Zdziarski, Johnson & Magdziarz 1996), with photon index constrained to be less than 3. We fix the electron temperature at 50 keV, outside the bandpass of the spectral fits, and the absorbing column at 1.2×10^{21} cm^{-2} (R07). We also add a Gaussian line and smeared edge to approximately account for the effects of reflection. We obtain good fits ($\chi^2/\nu < 1.25$) for all data sets.

Fig. 2 shows (open green triangles) the evolution of the photon spectral index of Comptonization. Using this information, together with the HID, and also by visually inspecting all energy and power spectra, we identify four distinct spectral states. The upper branch on the HID with hardness ratio ∼0.2 is characterized by strong disc emission, a weak high-energy tail and low rms variability, typical of the high/soft state behaviour. There is a short excursion to higher hardness ratios at a count rate around 1000 s^{-1} (MJD ∼53790), taking the system to the edge of a very high state, as also shown by the stronger variability including a transient quasi-periodic oscillation (QPO). The source then drops to very low hardness

---

[1] Publicly available as a local XSPEC model at http://heasarc.gsfc.nasa.gov/docs/xanadu/xspec/models/nthcomp.html.
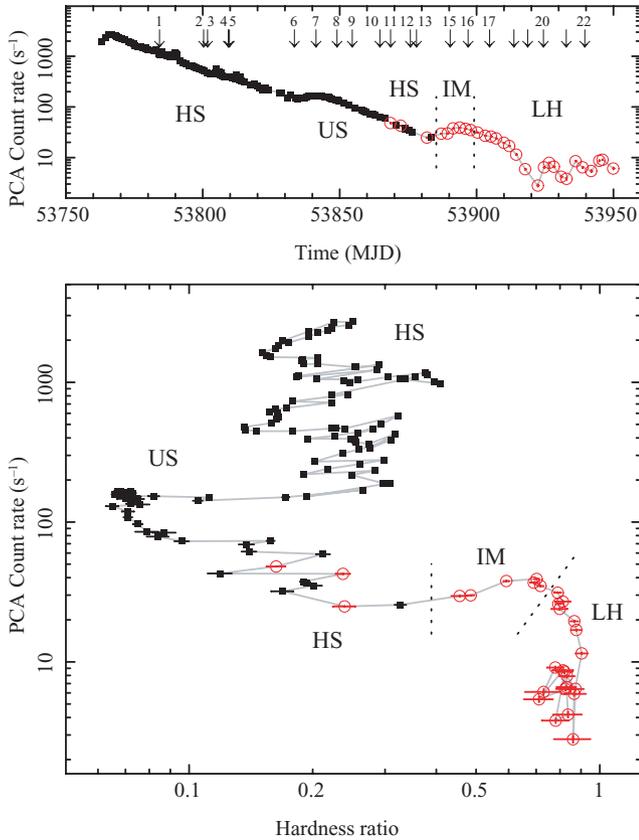
Figure 1. Light curve (upper panel) and hardness-intensity diagram for 2006 outburst of XTE J1817−330 from *RXTE* PCA data, detector 2 only. The dotted lines separate spectral states: HS – high/soft, IM – intermediate and LH – low/hard. US denote ultrasoft state, an extreme version of the high/soft state. Filled symbols represent PCA observations with well-established disc parameters. Open red circles show observations where either the disc was not statistically significant in the PCA data or the fractional error on its normalization was greater than 50 per cent. The arrows in the upper panel show times of *Swift* observations. The numbers above arrows show observation numbers, following R07 (only data with significant disc, see Tables 1 and 2).
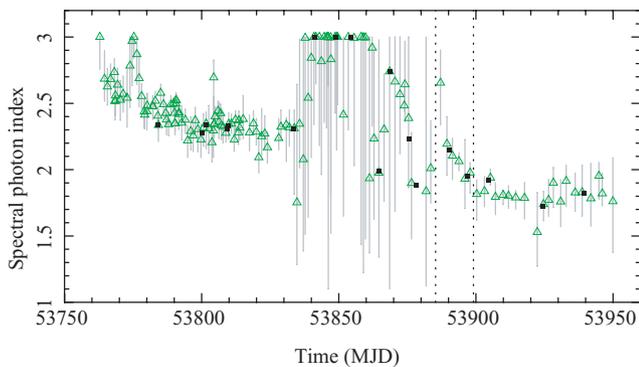
Figure 2. Evolution of the X-ray photon spectral index, Γ, during the outburst. Open green triangles show the best-fitting values from the *RXTE* PCA data. Filled black squares represent interpolated Γ used for *Swift* fits. The dotted lines represent onsets of the intermediate and hard states (see Fig. 1). The interpolated values of Γ are shown in Table 1.

ratios (≤ 0.1), sometimes termed an ultrasoft state but this is simply an extreme case of the soft state, with a low-temperature disc and a very weak high-energy tail.

The focus of this paper is the transition to the hard state in the later part of the outburst. The onset of the transition is marked by an increasing fraction of Comptonization giving increasing hardness ratio, and increasing rms variability. The transition is rather smooth so it cannot be pinpointed very accurately. We use a hardness ratio of 0.4 (and low count rate $<100\,\mathrm{s}^{-1}$ to distinguish from the very high state) to mark the beginning of the transition to an intermediate state, and the point where the spectral index becomes less than two as the beginning of the low/hard state. We use these boundaries to identify the X-ray spectral states for *Swift* data. Thus, observations 1–13 are in the soft state, 15 and 16 are intermediate spectra during the transition into the hard state, while later observations are in the hard state (see table 1 of R07).

3.2 Disc radius from a simple disc model

The results from the simple disc model are shown in Table 1. Fig. 3 shows the evolution of the disc parameters (temperature and radius) throughout the outburst as derived from the simple fits. We only include *RXTE* spectra for which the disc properties can be well constrained (we rejected the data where the uncertainty of normalization is more than 50 per cent of normalization itself). This selects *only* high state data, and excludes *all* the intermediate- and low-state data, which are the focus of this paper. The inner disc temperature drops from about 0.95 to 0.4 keV, throughout the soft states but the disc inner radius (proportional to square root of DISKBB normalization) remains remarkably constant. This is equivalent to saying that the disc flux, F and temperature, $T_{\rm in}$ closely follow the expected thermal relationship $F \propto T_{\rm in}^4$ from a constant emitting area, as shown in Fig. 4.

However, the lower limit of 3 keV on the low-energy bandpass of the PCA means that these data cannot constrain the disc properties of the soft-to-hard transition and the hard state. Lower bandpass

Table 1. Fit results of the simple disc model. $T_{\rm in}$ is the disc temperature at the inner radius, $N_{\rm disc}$ is the disc normalization, Γ is the fixed Comptonization spectral index interpolated from *RXTE* data (see also Fig. 2). The dotted horizontal lines separate the spectral states (HS above, IM in the middle, LH at the bottom) in the same way as dotted lines in the figures.

Observations	$kT_{\rm in}$ (keV)	$N_{\rm disc}$ ($\times 10^3$)	Γ	χ_ν^2/Degrees of freedom
1	0.89 ± 0.01	2.5 ± 0.1	(2.34)	588.2/539
2	0.796 ± 0.006	2.4 ± 0.1	(2.28)	606.3/527
3	0.779 ± 0.007	2.6 ± 0.1	(2.34)	519.0/494
4	0.701 ± 0.007	2.8 ± 0.1	(2.31)	534.7/487
5	0.71 ± 0.01	2.7 ± 0.1	(2.33)	477.2/451
6	0.59 ± 0.01	4.3 ± 0.3	(2.31)	331.0/316
7	0.62 ± 0.01	$3.3^{+0.2}_{-0.1}$	(3.00)	338.1/361
8	0.583 ± 0.015	3.5 ± 0.2	(3.00)	358.3/290
9	$0.592^{+0.008}_{-0.007}$	3.2 ± 0.1	(3.00)	344.9/339
10	0.516 ± 0.009	$3.7^{+0.3}_{-0.2}$	(1.99)	310.4/261
11	0.504 ± 0.005	4.3 ± 0.2	(2.74)	421.5/337
12	0.489 ± 0.003	4.2 ± 0.1	(2.23)	588.2/362
13	0.478 ± 0.003	3.7 ± 0.1	(1.88)	672.3/360
15	0.392 ± 0.004	4.7 ± 0.2	(2.15)	432.9/367
16	0.294 ± 0.003	10.1 ± 0.5	(1.95)	474.2/396
17	$0.225^{+0.004}_{-0.002}$	18 ± 1.5	(1.92)	393.0/307
20	0.18 ± 0.03	3^{+4}_{-2}	(1.72)	40.8/40
22	$0.185^{+0.017}_{-0.014}$	6^{+3}_{-2}	(1.82)	66.3/64
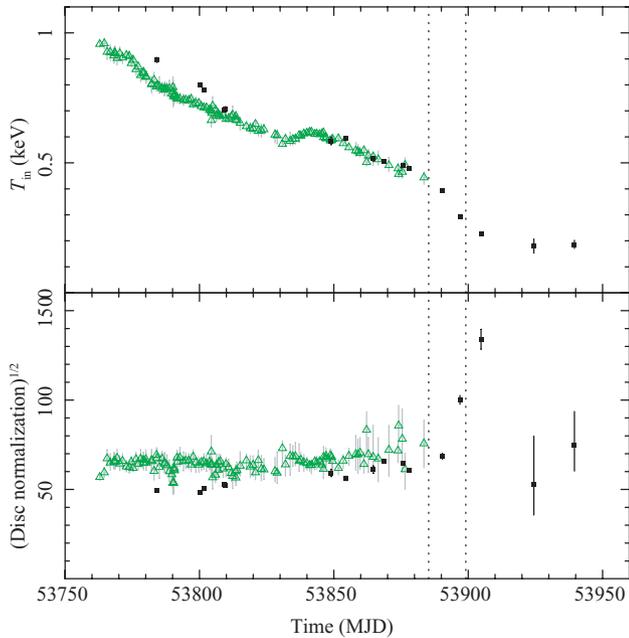
Figure 3. Temperature and square root of normalization (proportional to the inner disc radius) of the disc component. The green open triangles show the *RXTE* PCA data; only fit results with statistically significant disc and fractional error on its normalization less than 50 per cent are shown, hence no PCA data after ∼MJD 53875, where errors become very large. The black filled squares show the *Swift* XRT observations fitted with a standard disc model. The dotted lines represent onsets of the intermediate and hard states (see Fig. 1).
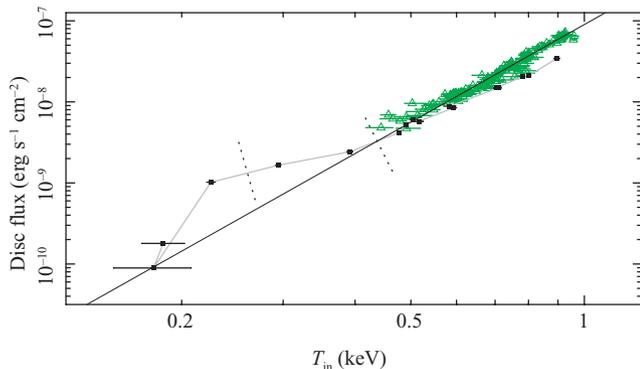
Figure 4. Disc flux as a function of disc temperature. The meaning of various symbols is the same as in Fig. 3. The dotted lines mark state transition, as in Fig. 1: HS is on the right-hand side, IS in the middle and LH state on the left-hand side. The straight line represents $F \propto T_{in}^4$ relation.

instruments (generally CCDs) are required, but these are often not easy to schedule for extensive monitoring campaigns. *Swift* carries perhaps the only CCD instrument for which the required sampling can be feasibly obtained, and the data set of R07 on XTE J1817−330 is outstanding in this regard, especially as this object has low Galactic absorption.

Ideally, the *Swift* 0.35–10 keV spectra could be fit together with quasi-simultaneous *RXTE* 3–20 keV data, however there is a small but significant change in spectral shape between the data sets which points to minor differences in calibration (probably enhanced to uncertainties in pileup correction at high luminosities). Instead, we fit only the *Swift* data, but fix the spectral index of the Comptonization to that seen in harder X-ray PCA data. As the *Swift* and *RXTE* data

are not quite simultaneous, we interpolate between the spectral indices measured from adjacent PCA observations. This should give a good estimate as Fig. 2 shows that the spectral index generally varies on time-scales of a few days, rather longer than the typical offset of less than a day between the *RXTE* and *Swift* observations. Fixing the spectral index reduces the number of free parameters in XRT fits, so helped to constrain the disc temperature and normalization. We also removed the reflection features from the model, as they are not required to fit the *Swift* data.

Most of the XRT spectra are well fit by this model, typically giving reduced $\chi_\nu^2 \sim 1$. The only exceptions are observations 12 and 13, where $\chi_\nu^2 = 1.62$ and 1.87, respectively. This is not due to the fixed Comptonization spectral index, as allowing this to be free leads to a very different type of fit. The spectrum is then dominated by a very low temperature/steep spectral index Comptonization component, in disagreement with the PCA data. This behaviour is typical of fitting a simple DISKBB model to more sophisticated (hence hopefully more realistic) disc spectra (Done & Davis 2008) as relativistic effects broaden the spectrum from that predicted by DISKBB, and the shape is made more complex by atomic features imprinted by radiative transfer through the vertical structure of the disc (e.g. Ebisawa, Mitsuda & Hanawa 1991; Zhang, Cui & Chen 1997; Davis et al. 2005; Li et al. 2005). Observations 12 and 13 are the ones with the highest signal-to-noise ratio (the source is brighter in earlier observations, but the pileup limits mean that the extracted count rate is smaller), so are the ones where this effect is most evident.

The results of these fits are shown in Figs 3 and 4 in black filled squares. The disc is not significantly detected in the XRT data sets 18, 19 and 21 (due mostly to poor signal-to-noise ratio as these are short exposures), so we exclude these from further analysis. There is a fairly good agreement between the disc derived from the PCA and XRT results in the soft state. Only the first five XRT observations (MJD 53784−53809) have slightly higher disc temperatures than corresponding PCA data, which again may be due to small differences in calibration between the PCA and XRT instruments, probably enhanced by uncertainties in pileup correction at these high count rates, and/or the different weighting of the DISKBB model fits to the different band passes (Done & Davis 2008).

The key aspect of the *Swift* data is that it extends the disc constraints into the spectral transition and hard state (Figs 3 and 4). These data clearly show that the inferred disc radius *increases* by a factor of ∼2 during the transition (XRT observations 15, 16 and 17). The same effect can be seen in tables 3 and 4 of R07, in clear confirmation of the predictions of the truncated disc model. However, the apparent disc inner radius then decreases in the hard state proper, back to a value which is consistent with the untruncated disc of the soft state (R07).

3.3 Irradiated disc model

The continuum model we used to fit XRT data in Section 3.2 consists of the two standard components expected in black hole spectra, namely the disc and its Comptonization by energetic electrons. They are linked to each other as the seed photons for Comptonization come from the disc, so any change in disc temperature affects the low-energy shape of Comptonization. However, the converse is not included: the simple models assume that Comptonization does not influence the disc.

This is plainly an approximation as the Comptonized component illuminates the disc. Some fraction of this illuminating

spectrum produces the reflected continuum and iron line, while the remaining, non-reflected, fraction is reprocessed and re-emitted as quasi-thermal emission and adds to the observed disc emission (e.g. Malzac, Dumont & Mouchet 2005). Where the disc is dominant energetically, the reprocessed emission from illumination from the Compton tail is only a small fraction of the intrinsic disc flux, so the observed disc spectrum consists mostly of its intrinsic emission. However, once the Compton tail carries a large fraction of the bolometric luminosity (as in the intermediate and especially hard states), the reprocessed emission can add substantially to the observed disc flux, affecting the inferred disc temperature, luminosity and hence radius.

We make a simple model of an X-ray illuminated disc. The fraction of Comptonized emission illuminating the disc is set by the solid angle of the reflector, $\Omega/2\pi$. The luminosity of the reprocessed emission is then $L_{rep} = \Omega/2\pi \, (1 - a) \, L_c$, where L_c is the luminosity in the Comptonized emission and a is the energy and angle integrated reflection albedo. This illumination adds to the intrinsic (gravitational) energy disc luminosity, L_d. Hence, the total observed disc luminosity is the sum of intrinsic and reprocessed luminosities, $L_d + L_{rep}$. We note that illumination alone underestimates the total heating expected in the truncated disc model, as the hot flow is in thermal contact with the disc, so there is also conductive flux from electrons (Meyer & Meyer-Hofmeister 1994; Różańska & Czerny 2000) and ions (Dullemond & Spruit 2005) which can also heat the disc.

Our model is designed to reproduce the standard DISKBB spectrum in the limits where the illuminating flux is negligible, so the intrinsic disc flux radial dependence is r^{-3} (i.e. has no stress-free inner boundary correction), with unilluminated disc luminosity L_d. A simple order of magnitude calculation shows that the reprocessed flux *dominates* the observed disc flux, i.e. $L_{rep} > L_d$, if $L_c/L_d \gtrsim 10$, at which point the observed ratio between the Compton tail and total disc emission is $L_c/(L_d + L_{rep}) \sim 5$. This holds for standard low/hard-state parameters of $\Omega/2\pi = 0.3$ and $a = 0.3$ (see e.g. Poutanen, Krolik & Ryde 1997; Gilfanov, Churazov & Revnivtsev 1999; Ibragimov et al. 2005).

The temperature structure of the illuminated disc is set by the (fourth root of the) sum of fluxes from the intrinsic and reprocessed emission at each radius in the disc. However, the radial dependence of the illumination which gives rise to the reprocessed flux is less easy to define than that for the intrinsic disc emission, as it depends on the relative geometry of the disc and Comptonization region. Motivated by the truncated disc scenario as sketched in Esin, McClintock & Narayan (1997) and DGK07, we consider especially the overlap region between the disc and hot flow which is required at the transition and in the bright low/hard states (Poutanen et al. 1997). Hence, we assume that the inner disc embedded in the hot flow is uniformly illuminated by the hot flow, and that the illumination of the rest of the disc is negligible. We scale this illumination radius, r_{irr}, in units of the inner disc radius.

We encode this model in XSPEC using THCOMP for the Comptonized emission. The model parameters are ratio of luminosities in Comptonization and unilluminated disc, L_c/L_d, and the irradiation radius r_{irr}. There are also Comptonization parameters, Γ, kT_e, and $\Omega/2\pi$ in addition to the unilluminated disc inner temperature, T_{in} and disc normalization proportional to the square root of the inner radius, $R_{in}^{1/2}$.[2]
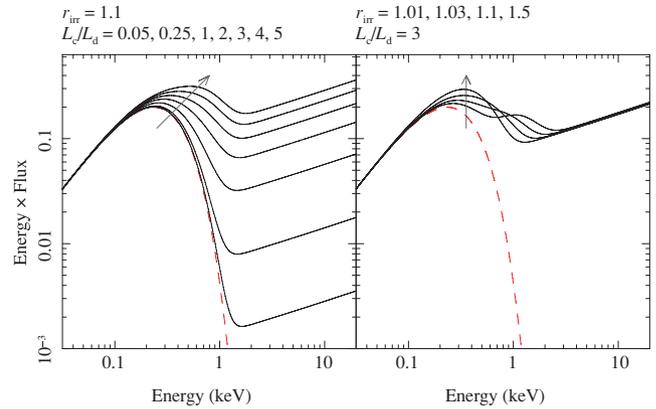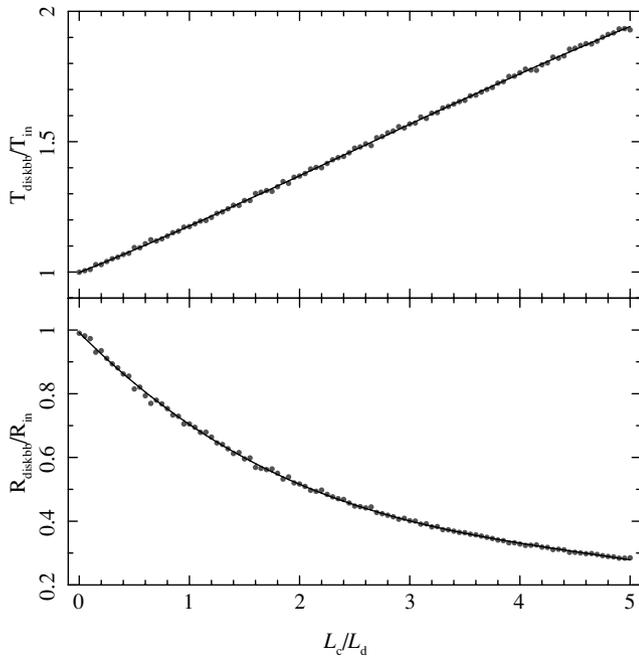

Figure 5. Model of the Compton-irradiated disc as a function of Compton-to-disc ratio, L_c/L_d (left-hand panel) and irradiation radius, r_{irr} (right-hand panel). The model was calculated for $kT_{in} = 0.1$ keV, $\Omega/2\pi = 0.3$, $\Gamma = 1.7$ and $kT_e = 100$ keV. The grey arrows show the direction of increasing L_c/L_d (left-hand panel) and r_{irr} (right-hand panel). The dashed line shows disc with no irradiation.

Fig. 5(a) shows a sequence of spectra of the irradiated disc model for increasing L_c/L_d for typical low/hard-state parameters and $r_{irr} = 1.1$ (Poutanen et al. 1997). The intrinsic disc remains the same throughout the sequence, i.e. there is the same accretion rate through a disc of constant radius. We also show the effect of changing the size of the irradiated region, r_{irr}, in Fig. 5(b). Obviously, the smaller this is, the higher the resulting temperature and vice versa. However, the amount of overlap also sets the Comptonized continuum shape, so this is *not* a free parameter (see Poutanen et al. 1997).

The disc spectrum is largely unaffected for $L_c/L_d < 1$. However, hard-state spectra have $L_c/L_d > 1$ where our models predict that the soft X-ray part of the spectrum deviates significantly from the original disc shape. There is a rise at soft energies resembling a disc spectrum, but it is significantly hotter than the underlying disc. If this is fit by a simple DISKBB model, the resulting temperature is higher and normalization (or radius) lower.

We quantify this effect by simulating a sequence of 100 spectra with L_c/L_d varying from 0 to 5 through the XRT response. We fit the simulated spectra by the same simple non-irradiated model of disc and Comptonization, we used in Section 3.2, and the resulting inferred temperature and inner radius are shown in Fig. 6. We stress again that the underlying disc in the simulated data has constant inner radius and mass accretion rate, yet its inferred temperature can be up to a factor of $\sim$2 higher in the hard state. More importantly, the measured, apparent inner radius coming out from spectral fits is *underestimated* by up to a factor of $\sim$3. This is crucial for the truncated disc model!

The factor by which the radius is underestimated depends on the strength of the irradiation, so depends also on the particular choice of $\Omega/2\pi$ and r_{irr} as well as on L_c/L_d. Increasing $\Omega/2\pi$ to 1 (as opposed to 0.3 in Fig. 6) increases the radius a few times in the limit of large L_c/L_d, while $r_{irr} = 1.5$ (as opposed to 1.1) increases the radius by a factor of $\sim$1.2–1.6. However, we stress again that these are not all independent factors. In a full model, the changing overlap geometry between the hot flow and cool disc, r_{irr}, sets the solid angle which determines both the amount of reflection, $\Omega/2\pi$ and the spectral index of the Comptonization. The reprocessed flux is then determined by the reflection albedo (so feeds back into the calculation of spectral index as it increases the seed photon flux) and

---

[2] This model, DISKIR, is publicly available on the XSPEC web page http:// heasarc.gsfc.nasa.gov/software/xspec.

Figure 6. Effect of irradiation on the disc measurements. The figure shows the standard, non-irradiated disc parameters, when it is fitted to a set of simulated data based on the irradiated disc. When there is no Comptonization ($L_c/L_d = 0$), both models provide the same results. However, with an increasing fraction of Comptonization and increasing irradiation, the disc becomes hotter (see Fig. 5). Fitting an irradiated disc with the non-irradiated model gives higher temperature and smaller inner radius. The grey points in the background show the actual fit results, while the black lines are third-order polynomial fits to these data. The data were simulated for $kT_{in} = 0.1$ keV, $\Omega/2\pi = 0.3$, $\Gamma = 1.7$, $kT_e = 100$ keV and $r_{irr} = 1.1$.

this is set by a combination of the ionization state of the disc (the disc is more reflective for high ionization) and the spectral index (high-energy photons cannot be reflected elastically due to Compton downscattering so $a < 0.3$ for hard spectra while $a \rightarrow 1$ for soft spectra reflected from a highly ionized disc). Such models with full coupled energetics (e.g. Malzac 2001; Malzac et al. 2005) are beyond the scope of this paper but we hope to address these in future work. Instead, here we simply set the irradiation parameters to those appropriate for a low/hard state with $\Gamma \sim 1.7$ (i.e. $\Omega/2\pi = 0.3$, $a = 0.3$, $r_{irr} = 1.1$: Poutanen et al. 1997). These are not appropriate for the soft state, but given that the reprocessed emission is negligible in these spectra then this has a little effect on the fits.

### 3.4 Spectral fits with the irradiated disc model

The results from fitting the data with our irradiated disc model are shown in Table 2. The disc inner radius as a function of the disc flux is shown in Fig. 7 in open red circles. Black filled squares show the results from non-irradiated DISKBB model, for comparison. As expected, in the soft state, where contribution from Comptonization, and irradiation, is weak, there is not much difference between the two models. The soft-to-hard-state transition, marked by a dotted line, begins when the disc flux drops below $\sim 3 \times 10^{-9}$ erg s^{-1} cm^{-2}. Even with the non-irradiated disc model, the inner disc radius increases by a factor of 2 during the transition, while with the irradiated model it increases by factor of 3, quantitatively but not qualitatively different. However, the two models give quite different results in the hard state, where the disc flux drops to $\sim 10^{-10}$ erg s^{-1} cm^{-2} (the corresponding bolometric flux is then about four times larger). While the non-irradiated model yields the inner disc radius comparable to that in the soft state, the irradiated model gives R_{in} about two to three times larger, and hence consistent with continuous truncation from the transition onwards.

Table 2. Fit results of the irradiated disc model. T_{in} is the intrinsic disc temperature at the inner radius, N_{disc} is the disc normalization, L_c/L_d is the ratio of luminosity in the Comptonized component to that in the non-irradiated disc (i.e. intrinsic disc emission). The dotted horizontal lines separate the spectral states in the same way as dotted lines in the figures.

Observations	kT_{in} (keV)	N_{disc} ($\times 10^3$)	L_c/L_d	χ^2_ν/Degress of freedom
1	0.88 ± 0.01	2.8 ± 0.1	0.12 ± 0.03	588.1/539
2	0.786 ± 0.007	2.6 ± 0.1	0.08 ± 0.01	606.6/527
3	0.771 ± 0.008	2.7 ± 0.1	0.06 ± 0.02	518.8/494
4	0.682 ± 0.008	3.3 ± 0.1	0.18 ± 0.02	531.9/487
5	0.69 ± 0.01	3.2 ± 0.2	0.18 ± 0.02	476.3/451
6	0.58 ± 0.01	$4.7^{+0.4}_{-0.3}$	0.1 ± 0.02	330.2/316
7	0.61 ± 0.01	$3.7^{+0.3}_{-0.2}$	0.07 ± 0.02	338.4/361
8	0.57 ± 0.02	4 ± 0.4	0.08 ± 0.03	358.6/290
9	0.589 ± 0.009	3.3 ± 0.2	0.02 ± 0.01	345.3/339
10	0.51 ± 0.01	4 ± 0.3	0.07 ± 0.02	309.4/261
11	0.498 ± 0.006	4.7 ± 0.2	0.06 ± 0.01	421.6/337
12	0.484 ± 0.004	4.4 ± 0.1	0.05 ± 0.01	584.4/362
13	0.472 ± 0.003	3.9 ± 0.1	0.08 ± 0.01	659.1/360
15	0.372 ± 0.005	6.2 ± 0.1	0.36 ± 0.02	417.2/367
16	$0.267^{+0.003}_{-0.004}$	$15.7^{+0.9}_{-0.8}$	0.68 ± 0.02	430.6/396
17	0.199 ± 0.004	31 ± 3	0.79 ± 0.03	373.5/307
20	$0.104^{+0.017}_{-0.014}$	27^{+26}_{-13}	$3.4^{+1.5}_{-0.8}$	40.1/40
22	$0.148^{+0.015}_{-0.013}$	16^{+9}_{-6}	1.2 ± 0.2	65.8/64
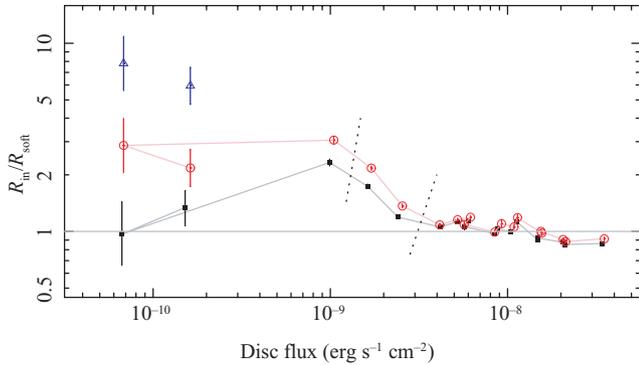
Figure 7. The inner disc radius, normalized to the mean radius in the soft state, as a function of the disc flux. Black filled squares represent the simple non-irradiated model (DISKBB); red circles show the Compton-irradiated model; blue triangles refer to the irradiated model with stress-free boundary condition (low/hard state only, observations 20 and 22). The dotted lines mark state transition, as in Fig. 1: HS is on the right-hand side, IS in the middle and LH state on the left-hand side.
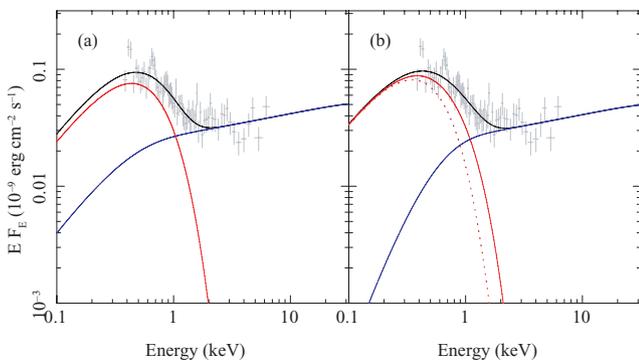
Figure 8. Unfolded and unabsorbed X-ray spectra of hard-state observation 22 (MJD 53939). The red curve (peaking at ∼0.4 keV) shows the disc, the blue curve (power law at higher energies) shows Comptonization, while the black curve corresponds to the sum of these. (a) Model with a standard non-irradiated disc. (b) Model with the irradiated disc; the dotted line shows the intrinsic emission of the disc from the gravitational heating. The solid red line shows the total disc emission, including contribution from Comptonization. In this model, the seed photons for Comptonization are assumed to be from the irradiated section of the disc only, so they have higher temperature and the low-energy cut-off in Comptonization is at higher energies in compare to the standard model.

In Fig. 8, we show that how the irradiated disc model differs from the standard, non-irradiated disc. In addition to the intrinsic emission from the disc from gravitational heating (dotted line in panel b), there is contribution from irradiation, which makes the disc hotter. When the same spectrum is fitted by the standard disc model (plus Comptonization), the disc temperature is overestimated and its inner radius underestimated.

The error bars in Fig. 7 are quite large and the recession of the disc in the hard state is not particularly significant. However, there are other aspects of the accretion disc structure which are different between this and the soft state. First, there is a stress-free inner boundary condition on a thin disc which extends down to the last stable orbit (e.g. Shakura & Syunyaev 1973), as supported by observations (e.g. DGK07). However, when the disc truncates at larger radii, then the stress should be continuous at the inner edge. Thus, a direct comparison of disc spectra between the soft

and hard states is not appropriate even without irradiation since they do not have the same stress condition in their inner boundary. The difference between a stressed and unstressed disc equates to the changes in inner radius by a factor of ∼2.7, hence to a truncation radius in the hard state of six to eight times that of the soft state. This corresponds to 40 or 50 gravitational radii.

Yet another issue which may lead to underestimation of the disc inner radius is Compton scattering. The hot plasma, which Compton scatters seed photons from the accretion disc, has optical depth of order unity. If this plasma lies in our line of sight to the disc then the observed disc emission is suppressed by a factor of ∼ exp (−τ), i.e., of the order of 2–3 (Kubota & Done 2004; Done & Kubota 2006). The total effect of this depends on geometry, but for the truncated disc/hot inner flow the seed photons are predominantly from the overlap region, so those on the far side of the black hole are strongly suppressed, especially in high-inclination systems, while those on the near side are not. Thus, this can make up to a factor of 2 decrease in disc flux i.e. a factor of $\sqrt{2}$ decrease in apparent disc inner radius (Makishima et al. 2008).

The irradiation (by definition) heats the top layer of the disc. This is unlikely to thermalize in the same way as the intrinsic gravitational energy release, which is dissipated deep within the disc. The irradiation flux most probably forms a moderately Comptonized spectrum, i.e. has a larger colour temperature correction than for the mostly thermalized soft-state emission. This effect alone would give rise to an decrease in apparent disc radius by a factor of $(f_{col,hard}/f_{col,soft})^2 \sim$ 1.5 if the colour temperature correction changes from $f_{col,soft} \sim 1.8$ in the soft state to $f_{col,hard} \sim 2.2$ for all the flux to be dissipated in the disc photosphere (Done & Davis 2008) in the hard state.

Where irradiation dominates the energetics, the resulting spectrum may be more complex than can be described by a single colour temperature corrected blackbody or disc blackbody. Davis et al. (2005) give two examples of spectra where half the energy is dissipated in the photosphere, showing clearly that the spectrum is much better described by Comptonization. This is very interesting as there is growing evidence that there is an additional component in the hard-state spectra. This component, a 'soft excess' of temperature higher than the disc, is required, in addition, to disc and high-temperature Comptonization in some hard-state spectra. It has been reported several times in Cyg X−1 (Ebisawa et al. 1996; Di Salvo et al. 2001; Ibragimov et al. 2005; Makishima et al. 2008) and in GRO J1655−40 (Takahashi et al. 2008). There is as yet no clear explanation for this component (see the list of possibilities in Di Salvo et al. 2001), but disc irradiation provides a physically plausible association. This is testable as it predicts that the variability of the reprocessed emission should follow that of the illuminating flux, with lag and smearing typical of the light travel time across the inner disc. This should also correlate with the variability of the iron line and reflected continuum, as the same irradiating flux produces both reprocessed and reflected emission.

A more complex spectrum for the soft emission may also potentially explain the apparent extremely broad iron lines which are sometimes inferred for the hard state. GX 339−4 is the best example of this, where the line derived for a low/hard state using simple continuum models requires a disc down to the last stable orbit of a rapidly spinning Kerr black hole, completely inconsistent with a truncated disc (Miller et al. 2006b). Incomplete thermalization of the reprocessed disc emission from irradiation means the spectrum extends up to higher energies than predicted by a blackbody disc, which could affect the red wing of the line. We will test this in a future paper, but here we note that such broad lines are now the only challenge to the truncated disc models for the hard state,

whereas there are multiple pieces of evidence which support them (e.g. DGK07).

4 CONCLUSIONS

In this paper, we demonstrate that the same data which are used by R07 to rule out the truncated disc model actually strongly support it. The transition spectra unambiguously show that the disc begins to recede as the source leaves the disc-dominated soft state (Fig. 7). The radius derived in the hard state is less robust, but we show that irradiation from the energetically dominant hot plasma can be crucial. The reprocessed flux from the hard X-ray illumination can dominate the intrinsic disc emission, leading to an underestimate of the disc radius by the factors of 2–3 (Fig. 6). Incorporating irradiation into the disc models gives hard-state radii which are consistent with the disc being truncated (Fig. 5). The inferred radius recedes still further when the potential difference in stress at the inner boundary, increased colour temperature correction from irradiation and loss of observable disc photons from Comptonization in the hot plasma are taken into account. We conclude that the inner disc radius in XTE J1817$-$330 in the hard spectral state is at least six to eight times that seen in the disc-dominated high/soft state, and that recession of the inner disc is the trigger for the soft-hard state transition, as predicted by the truncated disc models (Esin et al. 1997).

REFERENCES

Abramowicz M. A., Igumenshchev I. V., 2001, ApJ, 554, L53
Blandford R. D., Begelman M. C., 1999, MNRAS, 303, L1
Chaty S., Haswell C. A., Malzac J., Hynes R. I., Shrader C. R., Cui W., 2003, MNRAS, 346, 689
Churazov E., Gilfanov M., Revnivtsev M., 2001, MNRAS, 321, 759
Davis S. W., Blaes O. M., Hubeny I., Turner N. J., 2005, ApJ, 621, 372
Di Salvo T., Done C., Życki P. T., Burderi L., Robba N. R., 2001, ApJ, 547, 1024
Done C., Kubota A., 2006, MNRAS, 371, 1216
Done C., Davis S. W., 2008, ApJ, in press (arXiv:0803.0584)
Done C., Gierliński M., Kubota A., 2007, A&AR, 15, 1(DGK07)
Dullemond C. P., Spruit H. C., 2005, A&A, 434, 415
Ebisawa K., Mitsuda K., Hanawa T., 1991, ApJ, 367, 213
Ebisawa K., Ueda Y., Inoue H., Tanaka Y., White N. E., 1996, ApJ, 467, 419
Esin A. A., McClintock J. E., Narayan R., 1997, ApJ, 489, 865
Fender R. P., Belloni T. M., Gallo E., 2004, MNRAS, 355, 1105
Gilfanov M., Churazov E., Revnivtsev M., 1999, A&A, 352, 182
Ibragimov A., Poutanen J., Gilfanov M., Zdziarski A. A., Shrader C. R., 2005, MNRAS, 362, 1435
Kubota A., Done C., 2004, MNRAS, 353, 980
Li L.-X., Zimmerman E. R., Narayan R., McClintock J. E., 2005, ApJS, 157, 335
Makishima K. et al., 2008, PASJ, in press (arXiv:0801.3315)
Malzac J., 2001, MNRAS, 325, 1625
Malzac J., Dumont A. M., Mouchet M., 2005, A&A, 430, 761
Meyer F., Meyer-Hofmeister E., 1994, A&A, 288, 175
Miller J. M., Homan J., Miniutti G., 2006a, ApJ, 652, L113
Miller J. M., Homan J., Steeghs D., Rupen M., Hunstead R. W., Wijnands R., Charles P. A., Fabian A. C., 2006b, ApJ, 653, 525
Narayan R., Yi I., 1994, ApJ, 428, L13
Narayan R., McClintock J. E., 2008, New Astron. Rev., 51, 733
Poutanen J., Krolik J. H., Ryde F., 1997, MNRAS, 292, L21
Różańska A., Czerny B., 2000, A&A, 360, 1170
Rykoff E. S., Miller J. M., Steeghs D., Torres M. A. P., 2007, ApJ, 666, 1129 (R07)
Shakura N. I., Syunyaev R. A., 1973, A&A, 24, 337
Shapiro S. L., Lightman A. P., Eardley D. M., 1976, ApJ, 204, 187
Takahashi H. et al., 2008, PASJ, 60, 69
Zdziarski A. A., Johnson W. N., Magdziarz P., 1996, MNRAS, 283, 193
Zhang S. N., Cui W., Chen W., 1997, ApJ, 482, L155

This paper has been typeset from a TeX/LaTeX file prepared by the author.